ISSN 1674-1056
http://cpb.iphy.ac.cn
http://iopscience.iop.org/cpb
中国物理 B
Chinese Physics
中国物理
Chinese Physics B

Structure, stability, catalytic activity, and polarizabilities of small iridium clusters

Francisco E Jorge, José R da Costa Venâncio
Citation: Chin. Phys. B . 2018, 27(6): 063102. **doi:** 10.1088/1674-1056/27/6/063102

Journal homepage: http://cpb.iphy.ac.cn; http://iopscience.iop.org/cpb

What follows is a list of articles you may be interested in

Determination of static dipole polarizabilities of Yb atom

Zhi-Ming Tang(唐志明), Yan-Mei Yu(于艳梅), Chen-Zhong Dong(董晨钟)
Chin. Phys. B . 2018, 27(6): 063101. **doi:** 10.1088/1674-1056/27/6/063101

Relativistic and distorted wave effects on Xe 4d electron momentum distributions

Minfu Zhao(赵敏福), Xu Shan(单旭), Shanshan Niu(牛姗姗), Xiangjun Chen(陈向军)
Chin. Phys. B . 2017, 26(9): 093103. **doi:** 10.1088/1674-1056/26/9/093103

Dipole (hyper) polarizabilities of neutral silver clusters

Francisco E Jorge, Luiz G M de Macedo
Chin. Phys. B . 2016, 25(12): 123102. **doi:** 10.1088/1674-1056/25/12/123102

Calculations of the dynamic dipole polarizabilities for the Li^+ ion

Yong-Hui Zhang(张永慧), Li-Yan Tang(唐丽艳), Xian-Zhou Zhang(张现周), Ting-Yun Shi(史庭云)
Chin. Phys. B . 2016, 25(10): 103101. **doi:** 10.1088/1674-1056/25/10/103101

Calculations on polarization properties of alkali metal atoms using Dirac-Fock plus core polarization method

Tang Yong-Bo, Li Cheng-Bin, Qiao Hao-Xue
Chin. Phys. B . 2014, 23(6): 063101. **doi:** 10.1088/1674-1056/23/6/063101

Structure, stability, catalytic activity, and polarizabilities of small iridium clusters*

Francisco E Jorge[1,2,†] and José R da Costa Venâncio[1]

[1] *Unidade Acadêmica de Física, Universidade Federal de Campina Grande,* 58429-900 *Campina Grande, Brazil*
[2] *Departamento de Física, Universidade Federal do Espírito Santo,* 29060-900 *Vitória, Brazil*

(Received 12 November 2017; revised manuscript received 13 March 2018; published online 10 May 2018)

At the second order Douglas–Kroll–Hess (DKH2) level, the B3PW91 functional in conjunction with the relativistic all-electron basis set of valence triple zeta quality plus polarization functions are employed to compute bond lengths, dissociation energies, vertical ionization potentials, and the highest occupied molecular orbital-lowest unoccupied molecular orbital energy gaps of the small iridium clusters (Ir_n, $n \leqslant 8$). These results are compared with the experimental and theoretical data available in the literature. Our results confirm the theoretical predictions made by Feng *et al.* about the catalytic activities of the Ir_4 and Ir_6 clusters. From the optimized geometries, DKH2 calculations of static electric mean dipole polarizabilities and polarizability anisotropies are also carried out. It is the first time that the polarizabilities of small iridium clusters have been studied. For $n \leqslant 4$, the mean dipole polarizabilities per atom present an odd–even oscillatory behavior, whereas from Ir_5 to Ir_8, they decrease with the cluster size increasing. The dependence of the polarizability anisotropy on the structure symmetry of the iridium cluster is verified.

Keywords: B3PW91 functional, all-electron basis sets, DKH2 calculations, iridium clusters, polarizabilities

PACS: 31.15.aj, 31.15.eg, 36.40.–c **DOI:** 10.1088/1674-1056/27/6/063102

1. Introduction

It is known that the transition metals have an incomplete sub-shell in the ground state and that the d sub-shell plays an important role in the properties of the clusters or the bulk materials formed from these elements.[1,2] In the last few years, many theoretical and experimental studies about the group VIII transition metal clusters[3–16] were reported in the literature. The latter studies showed that the stability as well as the catalytic activity and electromagnetic properties are dependent on the size and structure of the cluster. The relationship between the stability and the structure of a cluster is important to understand its catalytic performance.

Iridium is a third row transition metal with a $5d^76s^2$ valence electron configuration. As it is not easily corroded, it is appropriate to be used as the materials that undergo high temperature and pressure.[17,18] Small iridium clusters present catalytic activity on solid support.[19,20] The Hartree–Fock (HF) method and effective core potential (ECP) basis sets were employed to investigate the dependence of the catalytic behavior on the size of iridium clusters (Ir_n, $n = 4$, 6, 8, and 10).[21,22] Similar studies for the ruthenium, rhodium, palladium, iridium, and platinum clusters were carried out by Zhang *et al.* at the density functional theory (DFT) level of theory.[23] From this study, it was shown that the cubic geometries for the iridium clusters are preferred.

As we can note, there are innumerous articles in the literature about the stability and catalytic activity of small iridium clusters, but, to the best of our knowledge, there is no published information about the polarizabilities of these clusters.

Polarizability measures the distortion of the electronic charge distribution of a system due to the presence of an external electric field, and it is useful to understand the electronic properties of clusters. As it is sensitive to the number of electrons and the structure and shape of the cluster, it is extremely valuable in understanding this kind of system.

In earlier researches, it was observed that the mean dipole polarizabilities of adjacent clusters of nickel and niobium often exhibit large variations[24–26] and that these polarizability variations are considerably larger than those obtained for the alkali metal clusters.[27–31] The noble metals (Cu, Ag, and Au), which are sometimes associated with the transition metals, have the d sub-shells fully filled and only one electron in the s valence orbital. In contrast to the nickel and niobium metal clusters, the mean dipole polarizability variations of the copper, silver, and gold clusters[32–34] were verified, in general, to be significantly smaller than those of the lithium and sodium clusters.[35]

For the iridium clusters, no theoretical or experimental results of electric polarizabilities have been reported to date in the literature. Therefore, it is currently only possible to carry out theoretical studies of these properties. For a better understanding of the size dependency and the electronic structure of the ground state iridium clusters up to the octamer, static mean dipole polarizabilities ($\bar{\alpha}$) and polarizability anisotropies

*Project supported by the CNPq, CAPES, and FAPES (Brazilian Agencies).
†Corresponding author. E-mail: jorge@cce.ufes.br
© 2018 Chinese Physical Society and IOP Publishing Ltd

($\Delta\alpha$) are calculated in this article. The reliability of these results is confirmed by the minimum polarizability principle (MPP).[36–38] Not only polarizabilities, but also optimized geometries, binding energies (*BE*), vertical ionization potentials (*VIP*), and highest occupied molecular orbital(HOMO)–lowest unoccupied molecular orbital (LUMO) energy gaps (E_g) are employed in this work to clarify the structure, stability, and catalytic activity of small iridium clusters.

2. Computational details

As iridium is a heavy element, it is necessary to consider simultaneously both correlation and relativistic effects on iridium cluster property calculations. So, the computational time rises quickly with the cluster size increasing. To reduce the cost, some strategies have been employed. For example, relativistic ECP along with a valence basis set has been used with success in studying the metal cluster electronic structures. On the other hand, for small metal clusters, relativistic DFT with a high-quality all-electron basis set can be used instead of ECP.

At the second-order Douglas–Kroll–Hess (DKH2) level,[39–41] the Becke three-parameter for exchange and Perdew–Wang 91 for correlation (B3PW91) functional[42,43] in conjunction with the relativistic all-electron basis set of valence triple zeta quality plus polarization functions and one diffuse function of *d* symmetry (TZP+1d-DKH)[44] as well as with the augmented TZP-DKH (ATZP-DKH)[44] set are utilized in this work. These sets are available at different formats at http://qcgv.ufes.br// and they have successfully been used by us and also by other research groups to determine the electronic structures of atoms,[44] molecules,[45–49] and alkali metal and transition metal clusters.[32–35] In the same way, the efficiency of the B3PW91 functional in studies of metal clusters can be confirmed in Refs. [13], [32]–[34] and the references therein. Throughout the calculations, spherical harmonic Gaussian functions and the Gaussian 03 program[50] are used.

First, the geometries of the iridium clusters are optimized at the DKH2-B3PW91/TZP+1d-DKH level and, then, the binding energies, ionization potentials, and HOMO–LUMO energy gaps are computed at the same level of theory. Next, the DKH2-B3PW91/ATZP-DKH polarizabilities are evaluated. It is worth pointing out that for iridium clusters, it is the first time that all electrons have been taken into account in the calculations of these properties and that our results can be useful in checking the accuracy that can be achieved with ECP.

To compute the properties mentioned above, the following equations are used:

$$IP = E(N-1) - E(N), \tag{1}$$

$$E_g = E(\mathrm{LUMO}) - E(\mathrm{HOMO}), \tag{2}$$

and

$$BE = nE_{\mathrm{Ir}} - E_{\mathrm{Ir}n}, \tag{3}$$

where $E(N-1)$ and $E(N)$ are, respectively, the cluster energies containing $(N-1)$ and N electrons, and n is the number of iridium atoms. The mean dipole polarizability and polarizability anisotropy are defined, respectively, as

$$\bar{\alpha} = (\alpha_{zz} + \alpha_{xx} + \alpha_{yy})/3, \tag{4}$$

$$\Delta\alpha = (1/2)^{1/2}[(\alpha_{xx} - \alpha_{yy})^2 + (\alpha_{yy} - \alpha_{zz})^2 + (\alpha_{zz} - \alpha_{xx})^2]^{1/2}. \tag{5}$$

3. Results and discussion

3.1. Structure

It is known that the number of isomers rises quickly with the iridium cluster size increasing. Therefore, for clusters with five or more atoms, it becomes practically impossible to study all isomers to determine the most stable one. With the purpose of reducing the number of clusters to be investigated, the acquired experience in the construction of metal clusters has been used to choose the possible configurations. Besides, in order to predict correctly the spin states of the iridium clusters it is also indispensable to consider high spin states due to the ground state electronic configuration of the atom ($5d^76s^2$). Recently, the ground state geometries and spin states of small iridium clusters were well established through different theoretical approaches.[10,12,13,22,51] The point group symmetries and multiplicities determined in Refs. [10], [12], and [13] are used by us to optimize the geometries of the Ir_n ($n \leqslant 8$) clusters with the DKH2-B3PW91/TZP+1d-DKH model. The equilibrium geometries obtained with this procedure are displayed in Fig. 1, whereas the corresponding average bond lengths (R_{ave}) are shown in Table 1. For comparison, theoretical values calculated with other approaches are also included[10,12] in this table. From Fig. 1, one can note that the Ir_4 cluster, like Ru_4,[52] has a square planar structure, while the other larger iridium clusters have three-dimensional (3D) structures. We recall that the four atom clusters of Pt, Pd, and Rh prefer the tetrahedral structure.

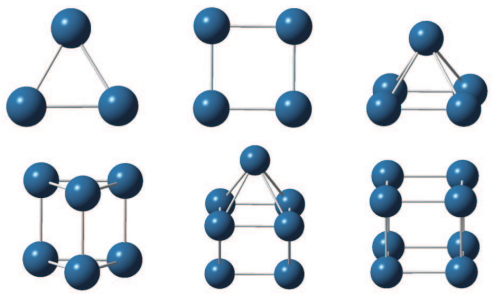


Fig. 1. (color online) Ground state structures of neutral iridium clusters, Ir_n (n = 3–8).

For the dimer, there is no experimental data available for the bond length and harmonic vibrational frequency. Nevertheless, Lombardi *et al.*[53] obtained indirectly 2.23 Å (Pauling's rule) and 280 cm^{-1}, which are in good agreement with our results (2.190 Å and 291.7 cm^{-1}).

For the trimer, we consider only the D_{3h} symmetry in accordance with Refs. [12] and [13]. In these references, scalar relativistic effects and the B3LYP and BPW91 functionals in conjunction with ECP valence basis sets are employed. In contrast, at the zero order regular approximation (ZORA) level, using the BP86 non-hybrid functional and the frozen-core triple-zeta basis sets plus polarization functions, Ping *et al.*[10] predicted C_{2v} symmetry for the ground state of Ir_3. The predictions obtained from the hybrid functionals are chosen by us because they are more reliable on cluster structure calculations. The R_{ave} value evaluated in this work (2.347 Å) is close to that obtained by Chen and Dixon[12] (2.389 Å).

For the tetramer, once again, whereas the B3LYP and BPW91 functionals predicted the D_{4h} symmetry for the ground state, the BP86 one is converged into the C_2 symmetry. The average bond lengths computed with the DKH2-B3PW91/TZP+1d-DKH (2.296 Å) and the relativistic B3LYP/aug-cc-pVDZ-pp (2.348 Å)[12] approaches agree well with each other.

For Ir_n ($n \geqslant 5$), our R_{ave} values are systematically smaller than those reported in Refs. [12] and [13] but, in general, in satisfactory agreement with them. Finally, we can note that the DKH2-B3PW91/TZP+1d-DKH average distances of all studied clusters do not exceed the experimental bulk bond length of 2.715 Å.

3.2. Stability

From the optimized geometries reported in Subsection 3.1, the values of *BE* of the iridium clusters are calculated and presented in Table 1. To assess the *BE* accuracy achieved in this work with the DKH2-B3PW91/TZP+1d-DKH model, the benchmark theoretical values, namely complete basis set (CBS) estimates obtained from CCSD(T)/aug-cc-pVNZ (N = D, T, Q, 5) calculations[12] are also included in this table.

For Ir_2, the DKH2-B3PW91/TZP+1d-DKH binding energy of 3.699 eV is in excellent accordance with the experimental data of 3.46 ± 0.12 eV[54] and 3.7 ± 0.7 eV.[55] Our *BE* agrees also with the CBS estimate of 3.799 eV.[12]

Table 1 shows that the DKH2-B3PW91/TZP+1d-DKH *BE*s increase with the cluster size increasing, and that except for Ir_5 and Ir_7, they are in excellent agreement with the CCSD(T)/CBS results.[12] From Ir_2 to Ir_8, we have also evaluated the binding energy per atom (BE/n), namely 1.850, 2.568, 3.013, 3.341, 3.765, 4.086, and 4.417 eV. Like *BE*, the BE/n rises with the iridium cluster size increasing. However, as the curve of BE/n versus n presents small peaks in the even-numbered clusters, this indicates that they are slightly more stable than the odd-numbered ones. When n goes to infinity, it is expected that the binding energy per atom comes close to the cohesive energy (6.94 eV)[56] of bulk iridium. Nevertheless, the BE/n of the Ir_8 cluster is yet far from the latter value. To reach 6.94 eV, it is necessary to consider larger clusters.

Table 1 displays the DKH2-B3PW91/TZP+1d-DKH vertical ionization potentials of the iridium clusters. This property reflects the ability of a cluster to lose an electron. Two general characteristics can be observed in Table 1: (i) Ir_2 presents the largest *VIP* value, (ii) from Ir_4 to Ir_8, the *VIP*s exhibit an odd–even oscillation characteristic with the maximum and minimum values occurring for the even- and odd-numbered clusters, respectively. This finding suggests once again that the even-numbered clusters are more stable than the nearest odd-numbered clusters.

For Ir, it is important to note that the experimental *VIP* of 8.967 eV[57] is in good accordance with our value of 8.690 eV. It suggests that the *VIP*s reported in this work seem to be reliable.

3.3. Catalytic activity

In Table 1, the DKH2-B3PW91/TZP+1d-DKH HOMO-LUMO energy gaps of the iridium clusters are shown. The HOMO–LUMO energy gap is a crucial parameter for studying electronic structures of molecules and clusters because it is associated with the chemical activity of the electronic system. In our case, a small E_g value points out that the iridium cluster is chemically active, whereas a large value indicates that the cluster is stable. In this article, the HOMO–LUMO energy gap will be used to measure the catalytic activity of a given cluster.

In Table 1, one can see that the first three clusters have the largest values of E_g and that, among them, Ir is the one that has the largest E_g value. In contrast, Ir_4 and Ir_6 have the smallest HOMO–LUMO energy gaps, consequently, they possess high reactivities. We recall that catalytic activities of these two clusters on solid support were observed previously.[19,20] From $n \geqslant 4$, Ir_8 exhibits the largest DKH2-B3PW91/TZP+1d-DKH HOMO–LUMO energy gap and it is at least twice as large as those of the tetramer and hexamer (cf. Table 1). Maybe, it can explain the possible low catalytic activity of the octamer. It also suggests that the octamer can be a stable cell to construct larger clusters. Feng *et al.*[22] studied Ir_n ($n = 4$, 6, 8, 10) clusters with the HF method and an ECP basis set, and verified that the reactivities of Ir_4 and Ir_6 without solid support are size-dependent, while Ir_8 and Ir_{10} can be of non-catalytic activity. The magnitudes of the E_g values calculated in this work are significantly smaller than those of Ref. [22]. It is not surprising, since these two theoretical approaches are completely different from one other. We take into account the electron correlation corrections and relativistic effects, whereas Feng *et al.* did not. In summary, our more reliable results add credence to the explanations of the iridium cluster reactivities, made by Feng *et al.* in 1997.

Table 1. Calculated values of average cluster bond length (R_{ave}), binding energy (BE), vertical ionization potential (VIP), and HOMO–LUMO energy gap (E_{gap}) for the ground state iridium clusters.

Cluster	Multiplicity	R_{ave}/Å		BE/eV		VIP/eV	E_{gap}/eV
		TZP+1d-DKH[a]	Literature	TZP+1d-DKH[a]	CBS[d]	TZP+1d-DKH[a]	TZP+1d-DKH[a]
Ir	4	–	–	–	–	8.690	2.562
Ir_2 ($D_{\infty h}$)	5	2.190	2.228[b]	3.699	3.799	9.472	2.262
Ir_3 (D_{3h})	4	2.347	2.389[b]	7.703	7.637	8.390	2.392
Ir_4 (D_{4h})	9	2.296	2.348[b]	12.051	12.645	7.586	0.851
Ir_5 (C_{4v})	8	2.418	2.431–2.538[c]	16.703	14.397	7.027	0.926
Ir_6 (D_{3h})	9	2.369	2.367–2.491[c]	22.591	23.742[c]	7.454	0.849
Ir_7 (C_{2v})	12	2.439	2.520[b]	28.605	26.196	7.420	1.491
Ir_8 (O_h)	13	2.364	2.429[b]	35.336	34.414	7.489	1.875

[a] This work (DKH2-B3PW91). DKH all-electron basis set from Ref. [43]. [b] B3LYP result from Ref. [12]. Using the aug-cc-pVDZ-pp basis set with the appropriate relativistic pseudopotential. [c] ZORA-BP86 result from Ref. [10]. The frozen-core triple-zeta basis set plus polarization functions was used. [d] Complete basis set estimates obtained from CCSD(T)/aug-cc-pVNZ (N = D, T, Q, 5) calculations. [12]

3.4. Polarizabilities

The static polarizability is closely associated with the structural characteristics and electronic properties of clusters. In this article, the static mean dipole polarizabilities, mean dipole polarizabilities per atom, and polarizability anisotropies of small iridium clusters are calculated for the first time and displayed in Table 2. The DKH2-B3PW91/ATZP-DKH model is employed.

For Ir, the unique value of $\bar{\alpha}$ available in the literature was obtained at the relativistic LDA level of theory.[54] This value (51 a.u.) is larger than ours (41.87 a.u.). It is not the first time that the LDA functional has overestimated the mean dipole polarizability result.[58] On the other hand, using the DKH2-B3PW91 method and the Sapporo-DKH3-QZP basis set augmented with diffuse functions ([12s10p8d5f3g2h]),[59] we obtain 43.37 a.u., which is in excellent agreement with our result.

Table 2 shows that the $\bar{\alpha}$ values increase with cluster size increasing, i.e., with the total number of electrons increasing. Similar characteristics are detected for the copper, silver, and gold clusters.[32–34] We can note that the mean dipole polarizabilities of the iridium clusters are, in general, slightly smaller than the corresponding ones of the gold clusters.[34]

For $n \leqslant 4$, the $\bar{\alpha}/n$ values present an odd–even oscillatory trend like the cases for the copper, silver, and gold clusters. This characteristic is related to the odd–even oscillations of the DKH2-B3PW91/ATZP-DKH HOMO-LUMO energy gaps (see Table 1). A cluster with higher E_g value is more stable, consequently, its mean dipole polarizability per atom decreases. This tendency is clearly seen in our results. As expected, the tetramer presents the largest value of $\bar{\alpha}/n$. The oscillatory trend ceases at $n = 4$ because a transition occurs from two-dimensional (2D) structures to more compact 3D structures. From $n \geqslant 5$, one can note a decrease of the mean dipole polarizability per atom with the cluster size enlargement, whereas with exception of the Ir_6 cluster, the HOMO–LUMO energy gaps increase. For Ir_6, the structure symmetry (D_{3h}) seems to be more important than E_g. We recall that for $n \geqslant 5$, the binding energy per atom rises with increasing the number of atoms in the cluster. It is an indication that clusters with strong bonds have minimum values of polarizabilities per atom, which is in accordance with the MPP.

Although the magnitude of the HOMO–LUMO gap is directly related to that of the polarizability, this is not the only dependence, there is the influence of the geometry as well. In fact, there is a competition between these two contributions which determines the polarizability value. It is known that a large HOMO–LUMO energy gap conduces to a chemical stabilization, but the chemical stability of a cluster also depends on highly symmetric 2D and 3D geometries, which contribute to a reduction of the static polarizability.

The above discussion can explain why the mean dipole polarizability per atom of Ir_3 is larger than that of Ir_6, even though the Ir_3 and Ir_6 clusters have similar symmetries (D_{3h}). The latter cluster has a more compact structure (3D) than the former one (2D). Similar reasoning explains the polarizabilities per atom, obtained for the Ir_4 (2D) and Ir_8 (3D) clusters. Going from Ir_3 to Ir_4, $\bar{\alpha}/n$ increases because the electrons in Ir_4 are less attracted by the nuclei than those in Ir_3, resulting in a more open structure. The opposite occurs when a similar analysis is carried out with Ir_6 and Ir_8.

The polarizability anisotropy measures the deformation of the charge distribution due to the presence of an external electric field. A decrease of this property is an indication that the charge distribution is more spherically symmetric.

It is interesting to point out that there is an abrupt fall of the polarizability anisotropy going from the dimer to the trimer (cf. Table 2). This occurs because Ir_3 has a more compact structure than Ir_2. We recall that these clusters belong to the D_{3h} and $D_{\infty h}$ point groups, respectively. From the tetramer to the pentamer, another polarizability anisotropy reduction is observed. This happens due to a transition from a 2D structure to a 3D structure. The Ir_6 cluster has D_{3h} symmetry, and like Ir_3 it has a small polarizability anisotropy value. Finally, the

octamer has a highly symmetrical structure (O_h point group), consequently, its polarizability anisotropy goes to zero, indicating that it is the most compact cluster studied in this work.

Table 2. Values of static electric mean dipole polarizability ($\bar{\alpha}$), mean dipole polarizability per atom ($\bar{\alpha}/n$), and polarizability anisotropy ($\Delta\alpha$) for the ground state iridium clusters. All values are in unit a.u.

Cluster	ATZP-DKH[a]		
	$\bar{\alpha}$	$\bar{\alpha}/n$	$\Delta\alpha$
Ir	41.87	41.87	0.14
Ir_2	85.55	42.77	69.25
Ir_3	117.24	39.08	36.20
Ir_4	181.30	45.33	101.03
Ir_5	199.90	39.98	72.01
Ir_6	226.91	37.82	24.82
Ir_7	257.03	36.72	60.91
Ir_8	277.28	34.66	0.00

[a] This work (DKH2-B3PW91). All-electron basis set taken from Ref. [43].

It must be mentioned here that the DKH2-B3PW91/ATZP-DKH polarizability anisotropy of Au_3 (122.39 a.u.) reported in Ref. [34] is larger than that of Ir_3. The main reason for this significant difference is that, unlike Ir_3, it belongs to the C_{2v} point group, i.e., Au_3 has a more open structure. As the gold clusters with $n \geqslant 4$ are planar, differently from the iridium clusters, their $\Delta\alpha$ values increase with the number of atoms increasing.[34]

4. Conclusions

In this article, the DKH2-B3PW91/TZP+1d-DKH model has been employed to calculate geometries, binding energies, vertical ionization potentials, and HOMO-LUMO energy gaps of small iridium clusters.

In general, the DKH2-B3PW91/TZP+1d-DKH bond distances are in good agreement with results reported previously.[10,12] In particular, for Ir_2, our result is only 0.04 Å smaller than an experimental value found in the literature.[53]

Except for Ir_5 and Ir_7, the DKH2-B3PW91/TZP+1d-DKH binding energies agree well with theoretical values obtained from a higher level of theory [CCSD(T)/CBS].[12] Like *BE*, the BE/n increases with the cluster size increasing. The binding energies per atom indicate that the even-numbered clusters are slightly more stable than the odd-numbered ones. From tetramer to octamer, the vertical ionization potentials exhibit an even–odd oscillating feature, indicating one more time that the even-numbered clusters are more stable.

From the HOMO–LUMO relativistic results reported in this work, we verify that Ir_4 and Ir_6 are the most reactive clusters and that Ir_8 presents low chemical activity. These findings confirm the predictions made by Feng *et al.*[22] about the catalytic and non-catalytic activities of the tetramer, hexamer, and octamer, respectively.

As the DKH2-B3PW91/ATZP-DKH polarizabilities calculated in this work are unique, they can be used to calibrate upcoming DFT and/or *ab initio* calculations. For $n \leqslant 4$, the mean dipole polarizabilities per atom display an odd–even oscillation. It is the inverse of that observed for the HOMO–LUMO energy gaps. It is in accordance with the chemical intuition. As expected, the largest $\bar{\alpha}/n$ value occurs for the tetramer. Among the eight clusters studied here, the smallest polarizability anisotropy is found for Ir_8, which belongs to the O_h point group. This cluster has the most compact structure.

References

[1] Alonso J A 2000 *Chem. Rev.* **100** 637
[2] Baletto F and Ferrando R 2005 *Rev. Mod. Phys.* **77** 371
[3] Luo Y H, Ren F Z, Wang Y X, Wei S K and Zhang G B 2009 *Chin. Phys. B* **18** 1491
[4] Feng C J, Xue Y H, Zhang X C and Zhang X Y 2009 *Chin. Phys. B* **18** 1436
[5] Shi S P, Zhang C Y, Zhao X F, Li X, Yan M and Jiang G 2017 *Chin. Phys. B* **26** 083103
[6] Lv J, Zhang J Y, Liang R R and Wu H S 2016 *Chin. Phys. B* **25** 063103
[7] Chen Y, Huo M, Chen T, Li Q, Sun Z and Song L 2015 *Phys. Chem. Chem. Phys.* **17** 1680
[8] Xing X, Hermann A, Kuang X, Ju M, Lu C, Jin Y, Xia X and Maroulis G 2016 *Sci. Rep.* **6** 19656
[9] Bucher J P, Doaglass D C and Bloomfield L A 1991 *Phys. Rev. Lett.* **66** 3052
[10] Guo P, Zheng J M, Zhao P, Zheng L L and Ren Z Y 2010 *Chin. Phys. B* **19** 083601
[11] Bae Y C, Osanai H, Kumar V and Kawazoe Y 2004 *Phys. Rev. B* **70** 195413
[12] Chen M and Dixon D A 2013 *J. Phys. Chem. A* **117** 3676
[13] Du J, Sun X, Chen J and Jiang G 2010 *J. Phys. Chem. A* **114** 12825
[14] Omidvar A, RashidianVaziri M R, Jaleh B, Shabestari N P and Noroozi M 2016 *Chin. Phys. B* **25** 118102
[15] Cheng Z D, Zhu J and Tang Z 2011 *Chin. Phys. Lett.* **28** 037501
[16] Mi H, Wei S H, Duan X M and Pan X Y 2015 *Chin. Phys. B* **24** 098201
[17] Baldo M A, Thompson M B and Forrest S R 2000 *Nature* **403** 750
[18] Habar M, Ouannasser S, Stauffer L, Dreyssé H and Wille L T 1996 *Surf. Sci.* **352–354** 5
[19] Xu Z, Xiao F S, Purnell S K, Alexeev O, Kawi S, Deutsch S E and Gates B C 1994 *Nature* **372** 346
[20] Maloncy S D, van Zon F B M, Kelley M J, Koningsbegger D C and Gates B C 1990 *Caral. Lett.* **5** 161
[21] Hay P J and Wadt W R 1985 *J. Chem. Phys.* **82** 299
[22] Feng J N, Huang X R and Li Z X 1997 *Chem. Phys. Lett.* **276** 334
[23] Zhang W Q, Xiao L, Hirata Y, Pawluk T and Wang L C 2004 *Chem. Phys. Lett.* **383** 67
[24] Knickelbein M B 2001 *J. Chem. Phys.* **115** 5957
[25] Knickelbein M B 2003 *J. Chem. Phys.* **118** 6230
[26] Moro R, Xu X, Yin S and de Heer W A 2003 *Science* **300** 1265
[27] Knight W D, Clemenger K, de Heer W A and Saunders W A 1985 *Phys. Rev. B* **31** 2539
[28] Benichou E, Antoine R, Rayane D, Vezin B, Dalby F W, Dugourd Ph, Broyer M, Ristori C, Chandezon F, Huber B A, Rocco J C, Blundell S A and Guet C 1999 *Phys. Rev. A* **59** R1
[29] Rayane D, Allouche A R, Benichou E, Antoine R, Aubert-Frecon M, Dugourd Ph, Broyer M, Ristori C, Chandezon F, Huber B A and Guet C 1999 *Eur. Phys. J. D* **9** 243
[30] Antoine R, Rayane D, Allouche A R, Aubert-Frécon M, Benichou E, Dalby F W, Dougourd P, Broyer M and Guet C 1999 *J. Chem. Phys.* **110** 5568
[31] Tikhonov G, Kasperovich V, Wong K and Kresin V V 2001 *Phys. Rev. A* **64** 063202
[32] Jorge F E, Ferreira I B, Soprani D D and Gomes T 2016 *J. Braz. Chem. Soc.* **27** 127

[33] Jorge F E and de Macedo L G M 2016 *Chin. Phys. B* **25** 123102
[34] Jorge F E and Santos A S 2018 *J. Braz. Chem. Soc.* **29** 838
[35] De Souza F A L and Jorge F E 2013 *J. Braz. Chem. Soc.* **24** 1357
[36] Chattaraj P K and Sengupta S 1996 *J. Phys. Chem.* **100** 16126
[37] Chattaraj P K and Poddar A 1998 *J. Phys. Chem. A* **102** 9944
[38] Chattaraj P K and Poddar A 1999 *J. Phys. Chem.* **103** 1274
[39] Douglas M and Kroll N M 1974 *Ann. Phys.* **82** 89
[40] Hess B A 1985 *Phys. Rev. A: At. Mol. Opt. Phys.* **32** 756
[41] Hess B A 1986 *Phys. Rev. A: At. Mol. Opt. Phys.* **33** 3742
[42] Becke A D 1993 *J. Chem. Phys.* **98** 5648
[43] Perdew J P and Wang W R 1992 *Phys. Rev. B* **45** 13244
[44] Martins L S C, Jorge F E and Machado S F 2015 *Mol. Phys.* **113** 3578
[45] Jorge F E, de Oliveira A Z and Silva T P 2016 *Int. J. Quantum Chem.* **116** 21
[46] Antusek A and Sulka M 2016 *Chem. Phys. Lett.* **660** 127
[47] Novikov A S, Ivanov D M, Avdontceva M S and Kukushkin V Y 2017 *Cryst. Eng. Comm.* **19** 2517
[48] Galembeck S E, Caramori G F, Misturini A, Garcia L C and Orenha R P 2017 *Organometallics* **36** 3465
[49] Zhang Y, Miao H, Liu L, Zhang X and King R B 2017 *Polyhedron* **138** 194
[50] Frisch M J, Trucks G W, Schlegel H B, Scuseria G E, Robb M A, Cheeseman J R, Montgomery J A Jr, Vreven T, Kudin K N, Burant J C, Millam J M, Iyengar S S, Tomasi J, Barone V, Mennucci B, Cossi M, Scalmani G, Rega N, Petersson G A, Nakatsuji H, Hada M, Ehara M, Toyota K, Fukuda R, Hasegawa J, Ishida M, Nakajima T, Honda Y, Kitao O, Nakai H, Klene M, Li X, Knox J E, Hratchian H P, Cross J B, Adamo C, Jaramillo J, Gomperts R, Stratmann R E, Yazyev O, Austin A J, Cammi R, Pomelli C, Ochterski J W, Ayala P Y, Morokuma K, Voth G A, Salvador P, Dannenberg J J, Zakrzewski V G, Dapprich S, Daniels A D, Strain M C, Farkas O, Malick D K, Rabuck A D, Raghavachari K, Foresman J B, Ortiz J V, Cui Q, Baboul A G, Clifford S, Cioslowski J, Stefanov B B, Liu G, Liashenko A, Piskorz P, Komaromi I, Martin R L, Fox D J, Keith T, Al-Laham M A, Peng C Y, Nanayakkara A, Challacombe M, Gill P M W, Johnson B, Chen W, Wong M W, Gonzalez C and Pople J A 2003 *Gaussian* 03*, Revision A.1* (Pittsburgh: Gaussian, Inc.)
[51] Pawluk T, Hirata Y and Wang L 2005 *J. Phys. Chem. B* **109** 20817
[52] Zhang W, Zhao H and Wang L 2004 *J. Phys. Chem. B* **108** 2140
[53] Jules J L and Lombardi J R 2003 *J. Phys. Chem. A* **107** 1268
[54] Miedema A R and Gingerich K A 1979 *J. Phys. B: At. Mol. Phys.* **12** 2081
[55] Morse M D 1986 *Chem. Rev.* **86** 1049
[56] Kittel C 1986 *Introduction to Solid State Physics* (New York: Wiley and Sons)
[57] Lide D R (ed.) 2003 *CRC Handbook of Chemistry and Physics*, 84th edn. (Boca Raton, Florida: CRC Press)
[58] Roos B O, Lindh R, Malmqvist P ? A, Veryazov V and Widmark P O 2005 *Chem. Phys. Lett.* **409** 295
[59] Noro T, Sekiya M, Koga T 2013 *Theoret. Chem. Acc.* **132** 1363